42nd Annual Frequency Control Symposium - 1988

ENSEMBLE TIME AND FREQUENCY STABILITY OF GPS SATELLITE CLOCKS

by

David W. Allan and Trudi K. Peppler
Time and Frequency Division
National Bureau of Standards
Boulder, Colorado 80303

Abstract

In anticipation of cross-link ranging in the Global Positioning System (GPS) and the establishing of GPS ensemble time, we have investigated the frequency stability characteristics of the clocks in the constellation. Once those characteristics were ascertained we then optimally combined the clock readings using the NBS time scale algorithm software to generate a GPS space clock ensemble.

Frequency drifts of some parts in 10^{16} per day were observed in the GPS cesium beam frequency standards on board the space vehicles. The white noise frequency modulation (FM) in the cesium clocks gave rise to a daily time prediction error of only 8 to 10 ns. The long-term random deviations in the cesium clocks were nominally modeled by a flicker noise FM at a few parts in 10^{14} for $\sigma_y(\tau)$. The rubidium gas-cell frequency standards with no temperature control on their base plate showed significant frequency perturbations during the solar eclipse season. Because of this, these clocks were not included in the GPS space clock ensemble. Their short-term stability is better than the cesium clocks, but their long-term stability was characterized by a random-walk FM at about 1 part in 10^{13} at one day on a $\sigma_y(\tau)$ diagram. The rubidium clock with a temperature controlled base plate had a comparable long-term performance to the cesium clocks except for a much larger linear frequency drift and a rate of change of the frequency drift.

The GPS space clock ensemble frequency stability reached about 2 parts in 10^{14}. Not only is this comparable to some of the best clock ensembles at major timing centers throughout the world, but the calculated time dispersion for autonomous GPS performance has significant implications. The reference for this analysis was the NBS time scale.

Introduction and Procedure

The list of uses of the GPS has become very impressive and continues to increase. Aside from navigation, for which it was designed, the other main areas benefitting from the availability of GPS have been the geodesy and timing communities. The timing community has used GPS in two basic modes: 1) direct access to the GPS or UTC(USNO MC) time, which provides an accuracy of better than 100 ns [1], and 2) use of GPS in the common-view mode -- providing a time and frequency measurement capability between remote sites to about 10 ns in time and 1 part in 10^{14} for integration times longer than a few days [2,3]. It is the purpose of this paper to demonstrate a new and powerful usage of GPS by combining the readings of the free running and independent space vehicle (SV) clocks to generate a computed time scale better than the best clock in the system.

The motivation for this work has been two-fold: First, the GPS Joint Program Office (JPO) has plans to generate an ensemble time -- both for the master control station and for the GPS [4]. This paper demonstrates the quality available from the ensemble concept with real data from the SV clocks. The future quality should be significantly better with the full constellation of SV clocks. Second, it has been known for some time that some of the individual SV clock performances have been better in the space environment than when they were pre-launch tested on the ground. To have a calculated clock time better than the best one of these SV clocks in both the short and long term would be quite outstanding and would provide an independent time and frequency metrology tool for accessing the performance of earth bound clocks [5,6]. Of particular concern at the present time are annual variations in cesium clocks.

The performance of the individual SV clocks was characterized for both random and systematic behaviors against the free running NBS(AT1). All of the clocks had frequency drifts and these were subtracted. Table 1 shows the values of the frequency drifts removed. The short-term instabilities for the GPS cesium and rubidium clocks are well modeled by white noise FM, and the long-term instabilities by either flicker-noise or random-walk FM.

Once the random and systematic behavior of the clocks were characterized, the NBS time scale algorithm for generating NBS(AT1) and UTC(NBS) was used to generate a GPS SV space clock ensemble time [7-9]. The NBS time scale algorithm deals with both the short and the long term processes. Individual clock sigmas are estimated, from which adaptive weights are calculated. By optimizing the integration time constant for the adaptive weights, we can de-weight the clocks automatically during an abnormal frequency deviation. A constant is entered for each clock for the frequency updates, m_i, which is a function of both the white FM and of the flicker or random-walk FM models for that clock. The entrance and exit of each SV clock into or out of the ensemble is a function of the operational realities for each. The NBS algorithm is designed to deal with these entrances and exits with minimum perturbation to the ensemble time output.

GPS Clock Characteristics

Figures 1a and 1b are plots of the frequency and the frequency stability of NAVSTAR or SVN 3 (PRN 6). The eclipse periods are evident at 1/2 year spacings. This rubidium clock is well characterized by random walk FM in the long term.

Figures 2a and 2b are corresponding plots for NAVSTAR or SVN 4 (PRN 8). Again we see a very similar behavior as for SVN 3 for this rubidium clock.

Figures 3a and 3b are corresponding plots for NAVSTAR or SVN 6 (PRN 9). As a Block 1 rubidium clock, its performance is also very similar to SVN 3 and 4.

All of the above rubidium clocks had base plate temperature variations of a few degrees. The effect of the eclipse season on each of the clocks is clearly visible, but of a non-statistical nature. These clocks had adverse effects on the ensemble time output, and were therefore not included in the GPS space clock ensemble. Their long-term weighting factors were nearly negligible also; hence, their exclusion had no importance to the long-term stability of GPS ensemble time, which is one of the main points of this paper.

Figures 4a and 4b are corresponding plots for NAVSTAR or SVN 8 (PRN 11). Though this also was a rubidium clock, several upgrades were made on it over the previous rubidium clocks. One of the most important of which was to improve the temperature control for the clock's base plate from a few degrees to about 0.1 degree. These upgrades improved the long-term performance considerably, and reduced the effect of the solar eclipse seasons. The Block II SV rubidium clocks will have a similar base plate temperature control.

The time residuals for this clock were more nearly modeled by a cubic (drift of the frequency drift). Because the cubic makes long-term predictions difficult, we deliberately set the long-term time-constant for the frequency update low. We were then able to include this clock in the GPS space clock ensemble. The frequency drift was estimated from the minimum squared error of a quadratic fit to the frequency. This fitting process acts like a high pass filter, so the stability values for large τ values are biased low. The frequency drift on all of the other clocks was estimated using a second difference routine [11]. The long-term stability values are also biased low in this case, but not as much as for the removal of a cubic.

Figures 5a and 5b are corresponding plots for SVN 8 also, but for the cesium clock after switching from the rubidium clock. The rubidium clock was still demonstrating excellent frequency stability at the time of the change, but the switch to cesium occurred because of a failure in another part of the clock system.

Figures 6a and 6b are corresponding plots for NAVSTAR or SVN 9 (PRN 13).

Figures 7a and 7b are corresponding plots for NAVSTAR or SVN 10 (PRN 12).

Figures 8a, 8b, 8c, and 8d are corresponding plots for NAVSTAR or SVN 11 (PRN 3). Figures 8a and 8b are before the satellite was moved to a new position in the GPS constellation, and figures 8c and 8d are after the move.

Table 2 shows the starting parameters that were entered for each clock.

Results and Conclusions

Figures 9a and 9b are the frequency deviation and the frequency stability plots of the GPS SV ensemble time respectively with NBS(AT1) being the reference. The short term stability was modeled by a white-noise FM at $\sigma_y(\tau = 2 \text{ days}) = 3.7 \times 10^{-14}$, which corresponds to 2.6 ns (< 1 meter) rms GPS SV ensemble error contribution at 8 hours (the current nominal upload interval). Concerning 180 day autonomous operation performance capability, we estimate the GPS SV ensemble's rms error of prediction to be about 600 ns (180 m).

The primary cesium clock for the Federal Republic of Germany (PTB CS 1) was used along with NBS(AT1) to perform a three-cornered hat experiment in order to evaluate the independent stability of the GPS SV ensemble in its long-term performance. Table 3 gives the results.

We conclude that an optimum weighted combination of the times and frequencies from the GPS SV clocks can yield an ensemble output with outstanding performance both in the short-term as well as in the long-term integration times or prediction intervals. Some caution should be expressed, however, because even with about 800 days of data being analyzed, the confidence of the estimate for τ values of the order of a year is quite poor. Still it would appear that the use of such an approach in the future should be very beneficial to the system both in terms of performance and in terms of reliability and redundancy. Some caution also needs to be exercised in how the clocks are configured; for example, frequency steps in a clock can have some adverse effect on the ensemble performance. Research is being conducted to deal with this problem.

References

[1] W.J. Klepczynski, H.F. Fliegel, and D.W. Allan, "GPS Time Steering," Proc. of 18th Annual Precise Time and Time Interval (PTTI) Applications and Planning Meeting, Washington, D.C., Dec. 2-4, 1986, pp. 237-249.

[2] D.W. Allan, D.D. Davis, M.A. Weiss, A. Clements, B. Guinot, M. Granveaud, K. Dorenwendt, B. Fischer, P. Hetzel, S. Aoki, M.-K. Fujimoto, L. Charron, and N. Ashby, "Accuracy of International Time and Frequency Comparisons Via Global Positioning System Satellites in Common-View," IEEE Transactions on Instrumentation and Measurement, IM-34, 118-125 (1985).

[3] M.A. Weiss and D.W. Allan, "An NBS Calibration Procedure for Providing Time and Frequency at a Remote Site by Weighting and Smoothing of

GPS Common View Data," IEEE Trans. on I & M, IM-36, 572-578 (1987).

[4] F. Varnum, D.R. Brown, D.W. Allan, and T.K. Peppler, "Comparison of Time Scales Generated with the NBS Ensembling Algorithm," Proc. of the 19th Precise Time and Time Interval (PTTI) Planning Meeting, 1987.

[5] E. Bava, F. Cordara, V. Pettiti, and P. Tavella, "Analysis of the Seasonal Effects on a Cesium Clock to Improve the Long-Term Stability of a Times Scale," Proc. of the Annual Precise Time and Time Interval (PTTI) Applications and Planning Meeting, Redondo Beach, CA, Dec. 1-3, 1987, pp. 185-202.

[6] J.E. Gray, H.E. Machlan, and D.W. Allan, "The Effect of Humidity on Commercial Cesium Beam Atomic Clocks," Proc. of the 42nd Annual Symposium on Frequency Control, Baltimore, MD, June 1-3, 1988, to be published.

[7] D.W. Allan and M.A. Weiss, "The NBS Time Scale Algorithm, AT1," NBS Technical Note 1316.

[8] M.A. Weiss, D.W. Allan, and T.K. Peppler, "A Study of the NBS Time Scale Algorithm," submitted for publication in the Proc. of CPEM'88. Digest version published in 1988 Conf. on Precision Electromagnetic Measurements, Tsukuba Science City, Japan, June 7-10, 1988.

[9] D.W. Allan, M.A. Weiss, and T.K. Peppler, "In Search of the Best Clock," submitted for publication in the Proc. of CPEM'88. Digest version published in 1988 Conf. on Precision Electromagnetic Measurements (CPEM), Tsukuba Science City, Japan, June 7-10, 1988.

[10] D.A. Howe, D.A. Allan, and J.A. Barnes, "Properties of Signal Sources and Measurement Methods," Proc. of the 35th Annual Symposium on Frequency Control, 1981.

[11] D.W. Allan, "Time and Frequency (Time-Domain) Characterization, Estimation, and Prediction of Precision Clocks and Oscillators," IEEE Trans. on Ultrasonics, Ferroelectrics, and Frequency Control, UFFC-34, 647-654 (1987).

TABLE 1

SVN (PRN)	Mean Freq. (Parts in 10^{14})	Drift/day	Drift/day/day
3 (6)	-1285.7	-0.65	
4 (8)	4370.9	-3.27	
6 (9)	10861.0	-7.53	
6 (9)	1177.4	-5.07	
8 (11)	-931.6	-13.51	+0.0194
9 (13)	219.0	-0.02	
10 (12)	572.9	-0.07	
11 (3)	-54.4	-0.03*	
11 (3)	-69.9	-0.06	

*The frequency drift for this segment was sufficiently small that it was not subtracted before using the data in the GPS ensemble.

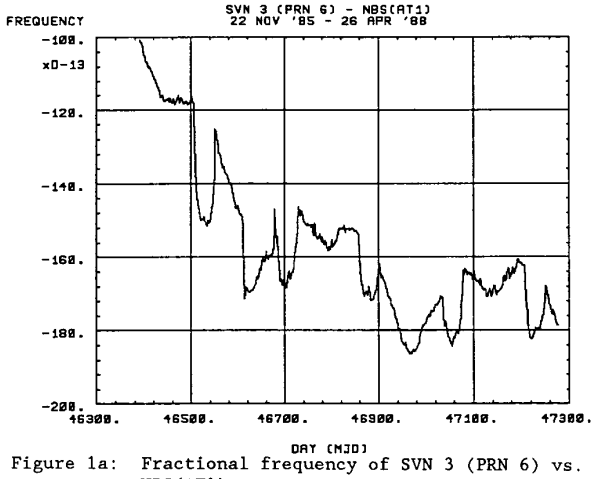

Figure 1a: Fractional frequency of SVN 3 (PRN 6) vs. NBS(AT1).

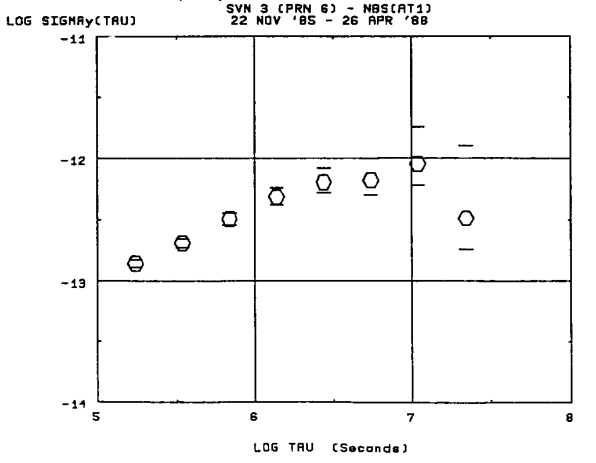

Figure 1b: Frequency stability of SVN 3 (PRN 6) after the drift was removed vs. NBS(AT1).

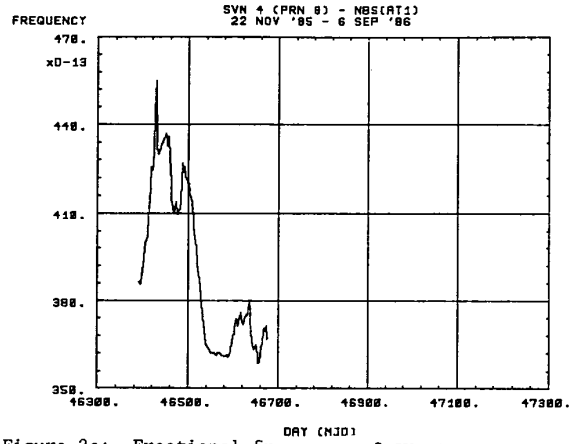

Figure 2a: Fractional frequency of SVN 4 (PRN 8) vs. NBS(AT1).

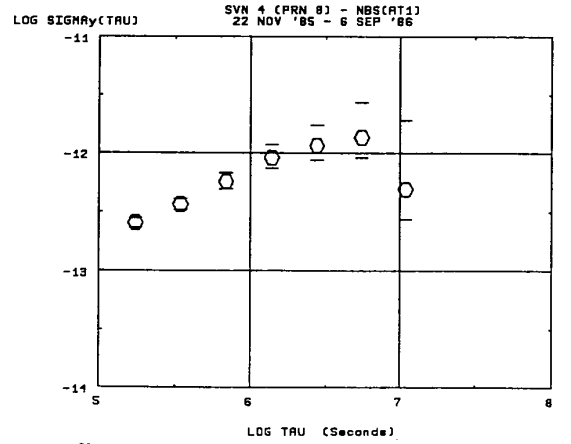

Figure 2b: Frequency stability of SVN 4 (PRN 8) after the drift was removed vs. NBS(AT1).

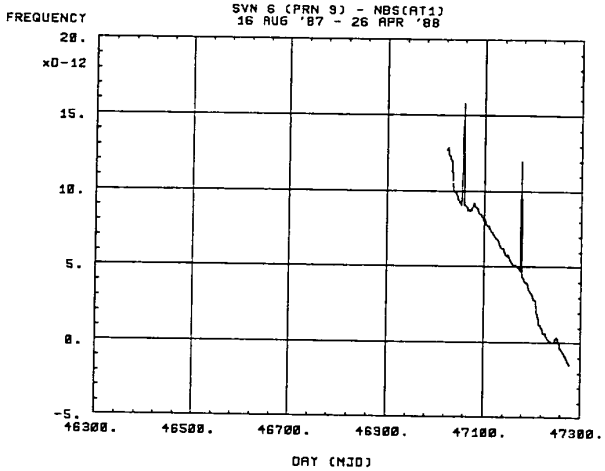

Figure 3a: Fractional frequency of SVN 6 (PRN 9) vs. NBS(AT1).

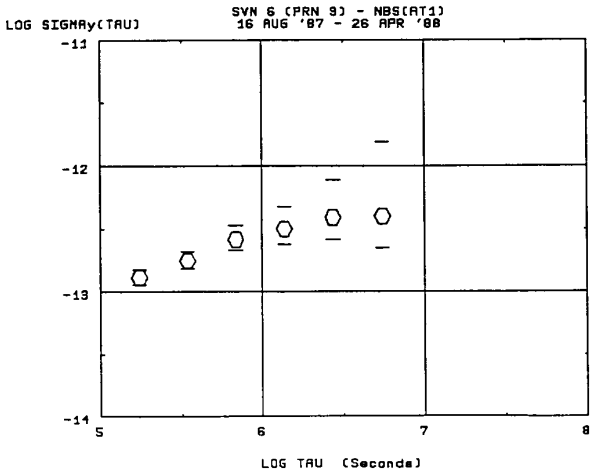

Figure 3b: Frequency stability of SVN 6 (PRN9) after the drift was removed vs. NBS(AT1).

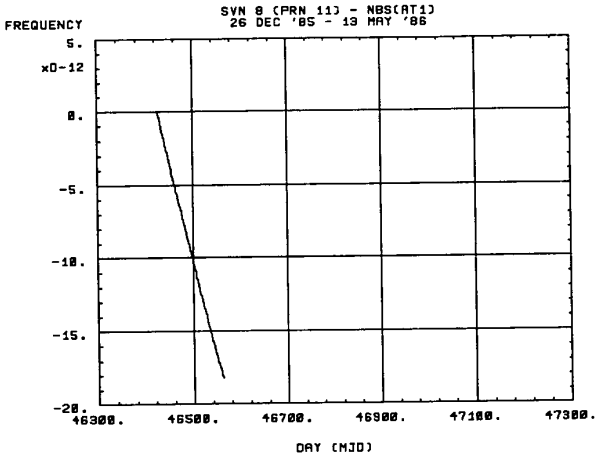

Figure 4a: Fractional frequency of SVN 8 (PRN 11) rubidium clock vs. NBS(AT1).

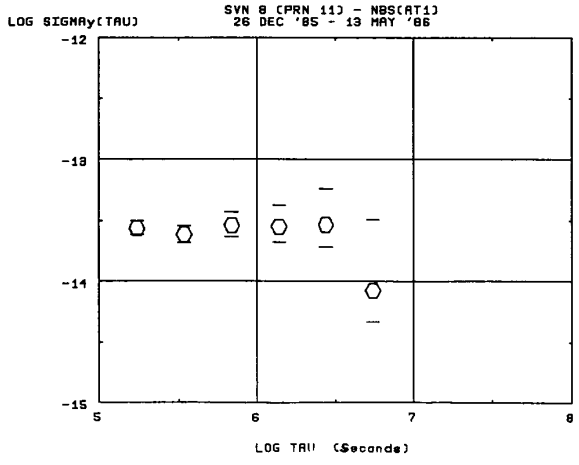

Figure 4b: Frequency stability of SVN 8 (PRN 11) rubidium clock after quadratic fit to frequency was removed vs. NBS(AT1).

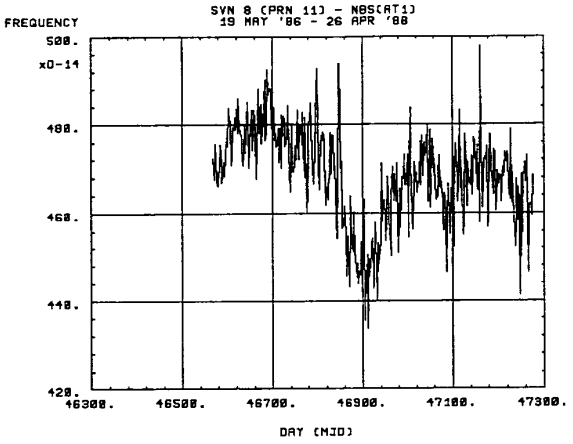

Figure 5a: Fractional frequency of SVN 8 (PRN 11) after switching to the cesium clock vs. NBS(AT1).

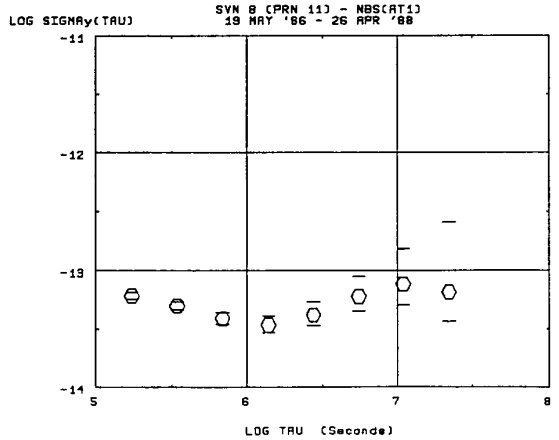

Figure 5b: Frequency stability of SVN 8 (PRN 11) after switching to the cesium clock and after the drift was removed vs. NBS(AT1).

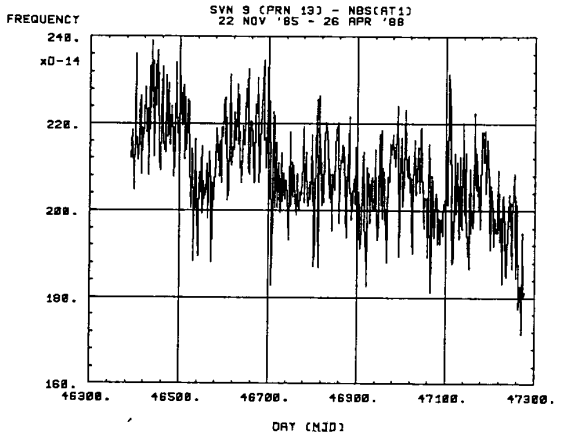

Figure 6a: Fractional frequency of SVN 9 (PRN 13) vs. NBS(AT1).

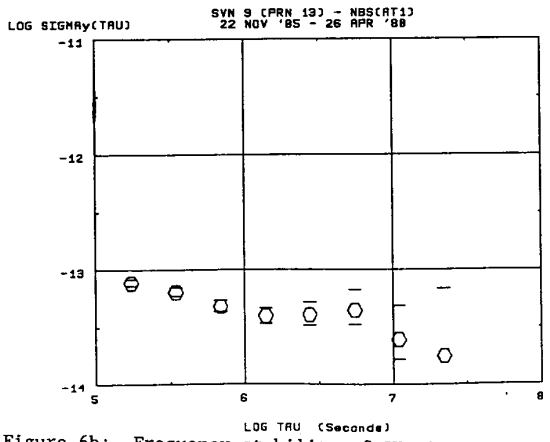

Figure 6b: Frequency stability of SVN 9 (PRN 13) after the drift was removed vs. NBS(AT1).

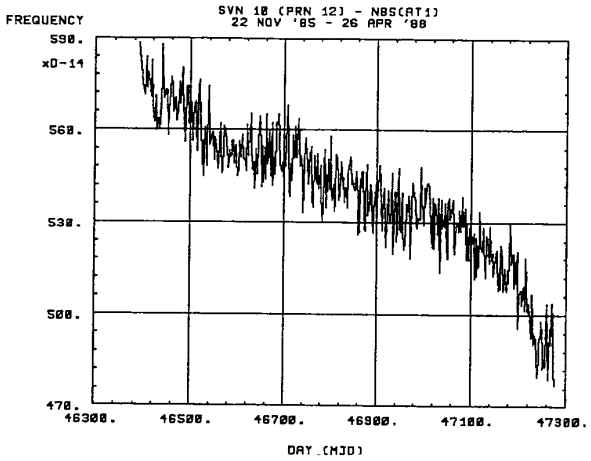

Figure 7a: Fractional frequency of SVN 10 (PRN 12) vs. NBS(AT1).

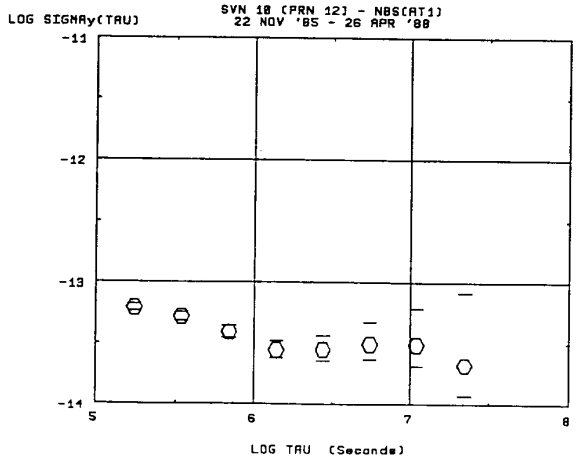

Figure 7b: Frequency stability of SVN 10 (PRN 12) after the drift was removed vs. NBS(AT1).

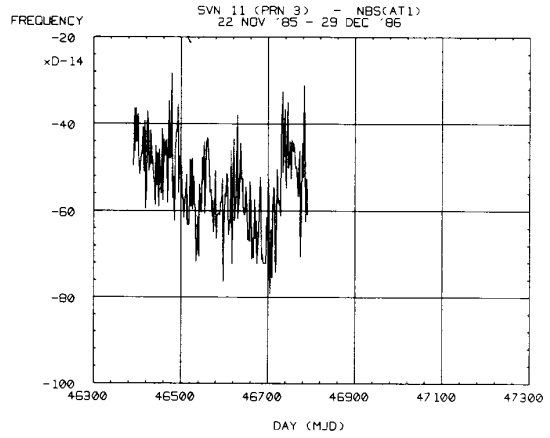

Figure 8a: Fractional frequency of SVN 11 (PRN 3) before the space vehicle was moved vs. NBS(AT1).

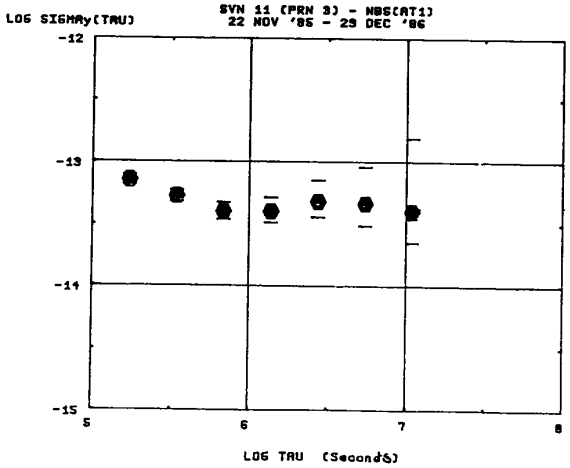

Figure 8b: Frequency stability of SVN 11 (PRN 3) with no drift removed and before the space vehicle was moved vs. NBS(AT1).

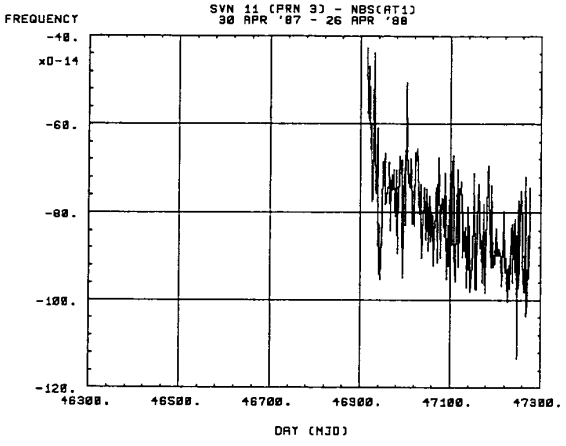

Figure 8c: Fractional frequency of SVN 11 (PRN 3) after the space vehicle was moved vs. NBS(AT1).

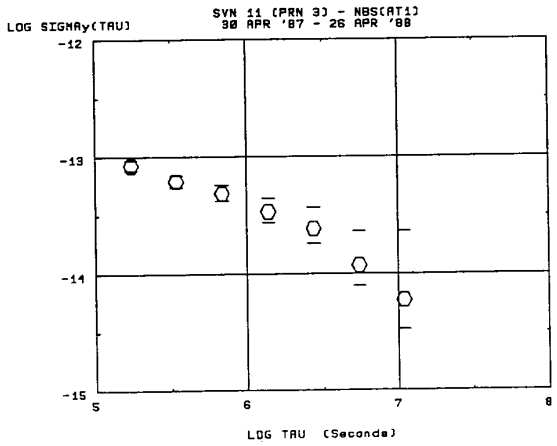

Figure 8d: Frequency stability of NBS 11 (PRN 3) after the drift was removed and after the space vehicle was moved vs. NBS(AT1).

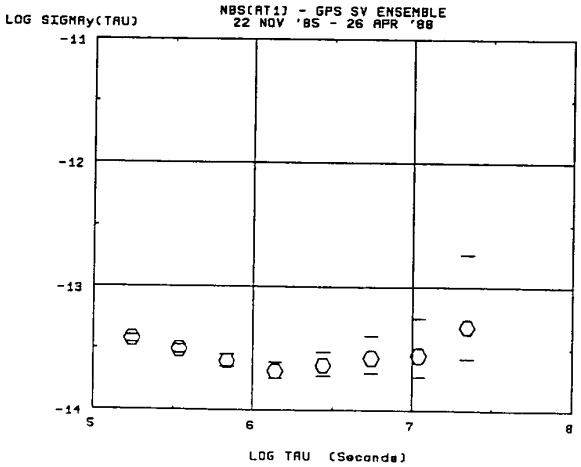

Figure 9b: Frequency stability of the GPS SV space clock ensemble vs. NBS(AT1).

TABLE 2

SVN (PRN)	Initial Clock Sigma at two-day prediction interval (ns)	Freq. update constant (m_i)
6 (9)	20.0	0.2
8 (11)	8.0	1.0
8 (11)	11.0	1.5
9 (13)	15.0	4.0
10 (12)	12.0	4.0
11 (3)	14.0	4.0
11 (3)	14.0	5.0

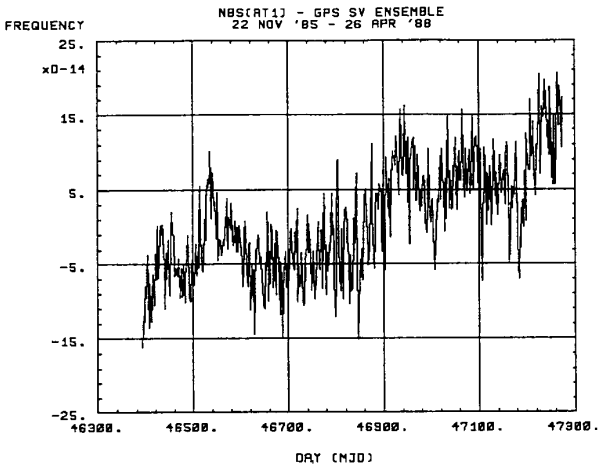

Figure 9a: Fractional frequency deviation of the GPS SV space clock ensemble vs. NBS(AT1).

TABLE 3

Frequency Stability, $\sigma_y(\tau)$ (Parts in 10^{14})

τ(days)	PTB(CS 1)	GPS SV ENSEMBLE	NBS(AT1)
10	2.0	2.1	0.9
20	1.6	2.0	0.3
40	1.9	2.3	**
80	2.5	2.9	**
160	2.8	3.7	**
320	4.0	6.3	**

**NBS(AT1) had a negative variance for these days as a result of the finite data length and the confidence of the estimates [10]. In a probablistic sense the negative variance implies that the instability of NBS(AT1) was less than either of the other two for these sample times, τ.